Aging Cell (2010) **9,** pp162–173 Doi: 10.1111/j.1474-9726.2009.00544.x

SIRT6 protects against pathological damage caused by diet-induced obesity

Yariv Kanfi,[1] Victoria Peshti,[1] Reuven Gil,[1] Shoshana Naiman,[1] Liat Nahum,[1] Eran Levin,[2] Noga Kronfeld-Schor[2] and Haim Y. Cohen[1]

[1]The Mina & Everard Goodman Faculty of Life Sciences, Bar-Ilan University, Ramat-Gan, Israel
[2]Deprtment of Zoology, Tel Aviv University, Tel Aviv, Israel

Summary

The NAD+-dependent SIRT6 deacetylase is a therapeutic candidate against the emerging metabolic syndrome epidemic. SIRT6, whose deficiency in mice results in premature aging phenotypes and metabolic defects, was implicated in a calorie restriction response that showed an opposite set of phenotypes from the metabolic syndrome. To explore the role of SIRT6 in metabolic stress, wild type and transgenic (TG) mice overexpressing SIRT6 were fed a high fat diet. In comparison to their wild-type littermates, SIRT6 TG mice accumulated significantly less visceral fat, LDL-cholesterol, and triglycerides. TG mice displayed enhanced glucose tolerance along with increased glucose-stimulated insulin secretion. Gene expression analysis of adipose tissue revealed that the positive effect of SIRT6 overexpression is associated with down regulation of a selective set of peroxisome proliferator-activated receptor-responsive genes, and genes associated with lipid storage, such as angiopoietin-like protein 4, adipocyte fatty acid-binding protein, and diacylglycerol acyltransferase 1, which were suggested as potential targets for drugs to control metabolic syndrome. These results demonstrate a protective role for SIRT6 against the metabolic consequences of diet-induced obesity and suggest a potentially beneficial effect of SIRT6 activation on age-related metabolic diseases.
Key words: diet-induced obesity; metabolic syndrome; SIRT6.

Introduction

Modern life is characterized by an increase in human longevity, accompanied by an increase in age-related metabolic diseases. One of the main epidemics of the twenty-first century is the metabolic syndrome. This syndrome includes a cluster of disorders comprising abdominal obesity, dyslipidemia, glucose intolerance, insulin resistance, and premature appearance of age-related diseases, such as diabetes type II, hypertension, generalized inflammation, and a propensity towards developing neurodegenerative diseases (Grundy *et al.*, 2005; Milionis *et al.*, 2008; Huang, 2009). The significant increase in human longevity along with the increasing prevalence of metabolic disorders creates medical challenges. To address these challenges, the mechanisms that determine the interplay between metabolism and aging must be better understood.

For more than 70 years, it has been known that calorie restricted (CR) diet slows the rate of aging and extends the life span of many organisms, including yeast and rodents (McCay *et al.*, 1935); (Weindruch & Walford, 1988). Moreover, rodents fed a CR diet display a spectrum of phenotypes that are the direct opposite of the metabolic syndrome, including decreased total body fat, LDL-cholesterol, free fatty acids (FFA) and triglycerides, improved glucose tolerance, and increased HDL-cholesterol. Additionally, the CR diet delays the appearance of many age-related disorders such as cancer, diabetes, and neurodegenerative diseases (Weindruch & Walford, 1988; Fontana & Klein, 2007). Thus, it is possible that metabolic syndrome and CR-associated changes lie at diametric ends of the same spectrum and involve an overlapping set of regulators (Guarente, 2006).

One family of proteins that have been implicated in aging and in the regulation of CR and the metabolic syndrome are the sirtuins. Sirtuins are highly conserved enzyme homologues of yeast Sir2, with NAD+ dependant deacetylase and/or mono ADP-ribosyltransferase activity (Imai *et al.*, 2000; Blander & Guarente, 2004; Liszt *et al.*, 2005; Haigis *et al.*, 2006). Studies in several organisms have indicated that sirtuins are critical in the regulation of longevity of *Saccharomyces cerevisiae* (Kaeberlein *et al.*, 1999), *Caenorhabditis elegans* (Tissenbaum & Guarente, 2001) and *Drosophila melanogaster* (Rogina & Helfand, 2004). In addition, mutations in ySir2 or Drosophila Sir2 block the beneficial effect of a CR diet on life span (Lin *et al.*, 2000; Rogina & Helfand, 2004). Thus, in these organisms, sirtuins are pivotal in regulating both longevity and the role of metabolism in life span.

There is much evidence to support a role for mammalian sirtuins (SIRT1 to 7) in CR and the metabolic syndrome (Guarente, 2006). Recent studies showed that nutrient levels and CR regulate the protein levels of SIRT1 and SIRT6 (Nemoto *et al.*, 2004; Kanfi *et al.*, 2008a,b). CR also regulates the anti-apoptotic activity of SIRT1 (Cohen *et al.*, 2004), and SIRT1$^{-/-}$ mice do not exhibit the increase in physical activity seen in wild-type (wt) mice under CR (Chen *et al.*, 2005). However, mice overexpressing SIRT1 or fed with SIRT1 activators such as resveratrol display only partial phenotypes of CR (Bordone *et al.*, 2007;

Correspondence
Haim Y. Cohen, The Mina & Everard Goodman Faculty of Life Sciences, Bar-Ilan University, Ramat-Gan 52900, Israel. Tel.: 972-3-531-8383; fax: 972-3-738-4058; e-mail: cohenh6@mail.biu.ac.il

Accepted for publication *8 December 2009*

Aging Cell

Pearson *et al.*, 2008). Thus, no single sirtuin is the sole player in CR-metabolic syndrome, and the identification of the role of other sirtuins in this pathway is required. Similarly, it was recently shown that mice overexpressing SIRT1 or fed with SIRT1 activators such as resveratrol are protected from metabolic damage induced by a high fat diet (HFD), through induction of antioxidant proteins and decreased activation of proinflammatory cytokines (Baur *et al.*, 2006; Pfluger *et al.*, 2008). It is unclear whether other sirtuins are involved in these responses, and whether the activation of other sirtuin family members will also protect against HFD.

SIRT6 has the potential to regulate the response to CR diet and the physiological effects of HFD. Recently we showed that SIRT6 protein levels increase in response to CR diet and nutrient limitation (Kanfi *et al.*, 2008b). The increase was due to stabilization of SIRT6 protein, and not via enhanced synthesis. These findings suggest that SIRT6 is involved in the beneficial effect of CR, that overexpression of SIRT6 might itself mimic CR, and that SIRT6 might be involved in the regulation of the metabolic syndrome.

SIRT6 was originally identified as ADP-ribosyltransferase; this is a nuclear protein that is found in association with chromatin, and is expressed in all of the tissues tested (Liszt *et al.*, 2005; Mostoslavsky *et al.*, 2006). A recent report showed that in addition to its ribosyltransferase activity, SIRT6 possesses a histone 3 (H3) lysine 9 deacetylase activity that modulates telomeric chromatin and cellular senesence (Michishita *et al.*, 2008). The precise role of SIRT6 in regulating metabolism is still elusive. SIRT6-deficient mice are small, express severe metabolic defects, and by 2–3 weeks of age develop abnormalities usually associated with aging. These abnormalities include profound lymphopenia, loss of subcutaneous fat, lordokyphosis, and eventually death at about 4 weeks (Mostoslavsky *et al.*, 2006). Notably, cells deficient in SIRT6 exhibit defects in base excision repair and are sensitive to oxidative stress. Serum insulin like growth factor 1 (IGF-1) and glucose levels are both severely reduced in SIRT6$^{-/-}$ mice by the age of 24 days (Mostoslavsky *et al.*, 2006). These findings suggest that SIRT6 is required for glucose homeostasis and maintenance of normal IGF-1 levels.

In this study, to follow a possible role for SIRT6 in the metabolic syndrome, we generated and characterized several lines of mice overexpressing exogenous SIRT6 (termed MOSES). When fed a standard chow diet, no significant difference was found in fat and glucose homeostasis between MOSES and wt littermates. Yet, under HFD, significant differences were found between the MOSES and their wt littermates including reduced accumulation of visceral fat, improved blood lipid profile, glucose tolerance, and insulin secretion, and reduced expression of selected peroxisome proliferator-activated receptor (PPAR)γ-regulated genes affecting lipid homeostasis. Taken together, these results demonstrate that SIRT6 overexpression protects against HFD-induced physiological damage by blocking the lipotoxicity of obesity, and restoring glucose homeostasis via specific reduction of PPARγ signaling and in the level of diacylglycerol acyltransferase 1 (DGAT1), a key regulator of triglycerides synthesis.

Results

Generation of transgenic mice

To follow a possible role for SIRT6 in metabolism, we generated the MOSES mice. SIRT6 cDNA was generated from mRNA isolated from the brain of a 3-month-old male mouse. The SIRT6 gene was cloned under the control of chicken beta actin promoter, and cytomegalovirus (CMV) enhancer (Fig. 1A). Eight founder mice were chosen, and the single integration site was verified by southern analysis. Throughout the study the viability rate of the MOSES mice was the same as their wt littermates. Overexpressed SIRT6 was detected by quantitative real-time PCR and western analysis in every tissue examined, including: heart, liver, pancreatic islets, white adipose tissue (WAT), muscle and brain (Fig. 1B and Table S1). Interestingly, the increased levels of SIRT6 resemble the observed increase in SIRT6 levels found in rats under CR (Kanfi *et al.*, 2008b), suggesting that MOSES mice may show beneficial physiological effects under HFD conditions.

SIRT6 overexpression protects against HFD-induced fat accumulation

Mice from three different lines, 85, 91, and 108, were fed *ad libitum* with normal chow diet. To follow a possible role for SIRT6 in HFD, mice were fed for 16 weeks with HFD in which 60% of

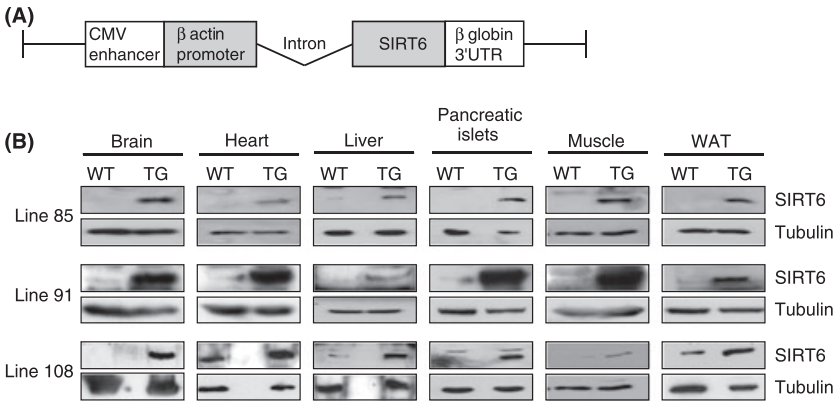

Fig. 1 Generation of transgenic (TG) mice. (A) Schematic representation of the 3.3 kb SIRT6 transgene construct. (B) Expression of SIRT6 in various organs of TG mice and their control wild-type littermates from lines 85, 91, and 108 analyzed by Western blot using a specific rabbit polyclonal antibody against SIRT6. WAT, white adipose tissue.

the calories were from fat, and metabolic parameters were measured. No difference was detected between the food intake of MOSES and their wt littermates, fed with chow or HFD, during 4 days of measurement (Fig. 2A). In addition, comparison between TG vs. wt mice showed no difference in the serum levels of the adipose derived hormone, leptin, which controls appetite (Fig. 2B). To estimate metabolic rate and substrate utilization, we measured oxygen consumption (VO_2) and carbon dioxide production (VCO_2), normalized to body weight. No difference was found between the TG mice and their wt littermates in either criterion (Fig. 2C). Similarly, there was no difference in the respiratory quotient (RQ, VO_2/VCO_2), indicating that both wt and TG mice use similar proportions of fat and carbohydrates as fuel substrates (Fig. 2C). Finally, no significant difference in body weight was found between the TG and their wt littermates (Fig. 2D).

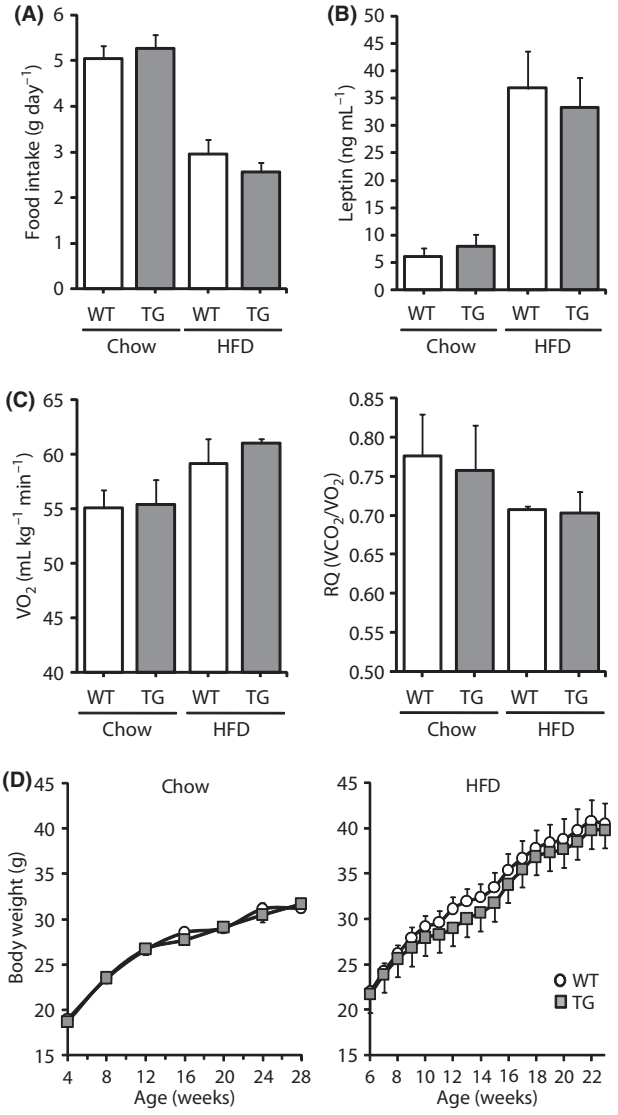

Fig. 2 Balanced Energy Homeostasis. (A) Food intake (g day^{-1}) of transgenic (TG) and wt mice fed with chow or high fat diet (HFD) (n = 5 per group; Chow: wt 5.05 ± 0.42, TG 5.26 ± 0.54; HFD: wt 2.95 ± 0.39, TG 2.56 ± 0.35; mean ± SEM). All measurements were carried out at the same time with mice at the same age. (B) Serum leptin levels of TG and wt mice fed with chow or HFD (n = 5–9 per group; mean ± SEM). (C) Oxygen consumption (VO_2) and respiratory quotient (RQ, VCO_2/VO_2) of TG and wt mice fed with chow or HFD (n = 5 per group; mean ± SEM). (D) Body weight of TG and wt mice fed with chow or HFD (chow, n = 18–30; HFD, n = 8–12 per group; mean ± SEM). For all values measured, no significant difference was found between TG and WT. Results were taken from line 85 and the other lines showed similar results.

Examining the body composition of the TG and wt mice, fed with normal chow diet, using dual-energy X-ray absorptiometry (DEXA) analysis showed no differences. Yet, when fed with HFD, MOSES mice had lower total body fat in comparison to their wt littermates (Fig. S1A,B) and an increase in total lean body mass (Fig. S1C). This increase in lean body mass probably explains the lack of significant difference in total body weight due to reduced fat content. Notably, weighing of visceral fat as a measurement of WAT content in three different lines showed a significant fat decrease of more than 25% in the TG mice in comparison to their wt littermates when fed HFD (Fig. 3A).

Obesity is also accompanied by an increase in triglycerides, FFA, LDL-cholesterol, LDL-/HDL-cholesterol ratio and lipidosis of the liver (fatty liver). No significant differences were found in the following general markers for liver lipidosis between the wt and MOSES mice: oil red O staining, weights and the levels of SREBP1 mRNA (data not shown and Fig. S2A,B). To follow the progression of lipidosis, liver slices of five TG and five wt littermates were examined for the presence of macro- and microvesiculars lipidosis, as the latter are associated with a worse prognosis in human patients (Burt *et al.*, 1998). All of the livers taken from wt animals had microvesicular lipidosis whereas only 20% of the TG mice were affected (Fig. S2C). In addition, the mRNA levels of interleukin 6 (IL-6) in the liver, a marker for inflammation, were lower in MOSES mice than in wt mice (Fig. S2D). Next, FFA, cholesterol, and triglyceride profile was measured in mice fed with chow diet or HFD. In mice fed with chow diet, there was no significant difference in the level of triglycerides between the wt and the TG mice (Fig. 3B). Yet, when fed HFD, MOSES mice showed 33% lower triglyceride levels than their wt littermates (Fig. 3B). Moreover, triglyceride levels in MOSES mice fed with HFD were similar to triglyceride levels of those fed with chow diet. Similarly, the TG mice accumulated 25% less FFA (Fig. 3C). Finally, when fed with either chow diet or HFD, the TG mice had significantly less LDL-cholesterol (50% and 30% respectively) in comparison to their wt littermates (Fig. 3D). Taken together, these results show that overexpressing SIRT6 attenuates the aberrations in fat homeostasis due to diet-induced obesity.

SIRT6 overexpression protects against impaired glucose tolerance induced by HFD

One of the hallmarks of the metabolic syndrome is a decrease in insulin sensitivity and the consequent development of impaired glucose tolerance. To follow the effect of overexpression of SIRT6 on glucose homeostasis, glucose levels were compared in

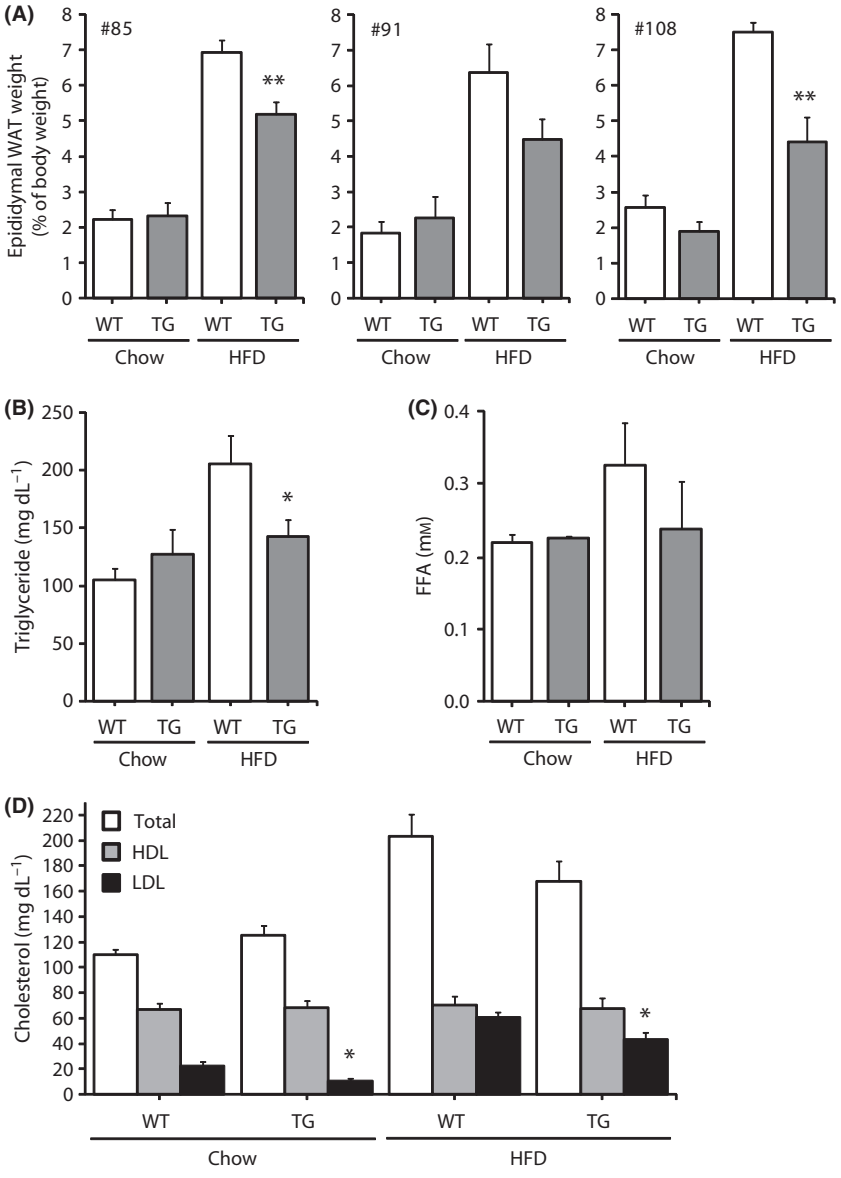

Fig. 3 Transgenic (TG) mice are protected against high fat diet (HFD)-induced fat accumulation. (A) Abdominal (epididymal) WAT weight as a percentage of body weight of TG and wt mice from lines 85, 91, and 108 fed with normal chow or HFD (WT, n = 7–12; TG, n = 5–8 per group; mean ± SEM). (B) Plasma triglyceride levels of TG and wt mice fed with chow or HFD (n = 9–12 per group, mean ± SEM). (C) Serum concentrations of free fatty acid of TG and wt mice fed with chow or HFD (n = 8 per group; mean ± SEM). (D) Plasma total cholesterol, LDL-cholesterol and HDL-cholesterol of TG and wt mice fed with chow or HFD (n = 8–11 per group; mean ± SEM). *P < 0.05, **P < 0.01. For B, C, and D results were taken from line 85 and the other lines showed similar results.

wild type and TG mice fed with normal chow diet. The TG mice had lower (although not significant) fasted glucose levels relative to their wt littermates (Fig. 4A). Lower glucose levels may suggest that the TG mice have more effective insulin signaling. To investigate this possibility, a glucose tolerance test (GTT) was performed on mice fed with chow or HFD. No difference was found in glucose uptake during the initial 2 h after glucose injection between the TG and wt littermates fed a normal chow diet (Fig. 4B). Strikingly, in mice fed with HFD in comparison to the wt mice, the glucose uptake in the TG mice was significantly more efficient in all three tested lines (Fig. 4C). Similarly, the calculated homeostasis model assessment (HOMA) measurement of insulin resistance was lower in TG mice fed with HFD (3.0 ± 0.2 in TG mice vs. 4.2 ± 0.9 in wt mice, mean ± SEM). To examine if the improved GTT is due to an increased insulin sensitivity, insulin secretion, or both, an insulin tolerance test (ITT) assay was performed; no significant difference was found in mice fed with chow diet or HFD (Fig. 4D). These results suggest that overexpression SIRT6 does not affect insulin sensitivity of the peripheral tissues. To explore the possibility that the TG mice secrete more insulin in response to glucose stimulus, we measured the insulin blood levels after glucose stimulation. As seen in Fig. 4E and Fig. S2F, under HFD but not chow diet (Fig. S2E) the TG mice secreted significantly higher levels of insulin upon glucose stimulation in comparison to their wt littermates. The enhanced glucose-stimulated insulin secretion (GSIS) was maintained *in vitro* in isolated pancreatic islets of TG mice, as compared to wt mice, 24 h following isolation (Fig. 4F). Chronic consumption of a HFD results in an increase in both peri- and intra–pancreatic fat, and inflammatory cells and is associated with high incidence of pancreatic inflammation in obese patients (Frossard *et al.*, 2009). Increased inflammation in

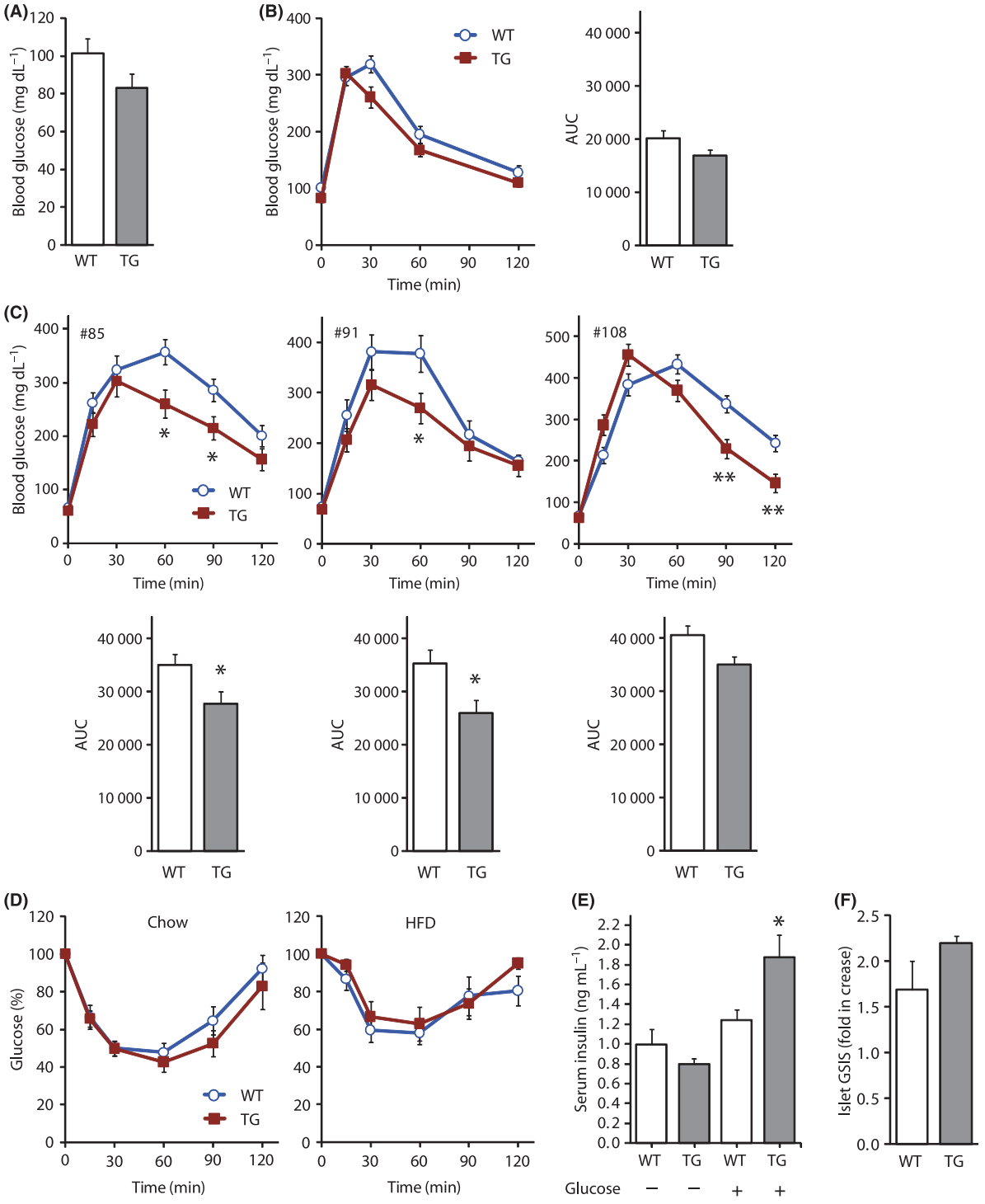

Fig. 4 Transgenic (TG) mice are protected against high fat diet (HFD)-Induced Glucose Intolerance. (A) Fasting blood glucose levels of TG and wt mice on chow diet (n = 7 per group, mean ± SEM). (B) Glucose tolerance test (GTT) (left) and area under curve (AUC) values (right) of TG and wt mice fed chow diet. Blood glucose was measured before the intraperitoneal injection of glucose (2 g kg^{-1} body weight), as well as at the times indicated after glucose administration (n = 7 per group, mean ± SEM). (C) GTT (upper) and AUC values (lower) of TG and wt mice fed with HFD from lines 85, 91 and 108 (WT, n = 5–13; TG, n = 7–9 per group, mean ± SEM). *P < 0.05, **P < 0.01. (D) Insulin tolerance test of TG and wt mice fed with chow or HFD. Blood glucose levels were determined before and at the times indicated after injection of insulin (0.75 U kg^{-1} body weight). Data are presented as percentage of initial blood glucose concentration (n = 5–8 per group, mean ± SEM). (E) Serum insulin levels of TG and wt mice, from line 85, fed with HFD before and 30 min after glucose administration (2 g kg^{-1} body weight) as measured by ELISA (n = 7–12 per group, mean ± SEM). *P < 0.03. (F) Glucose-stimulated insulin secretion of isolated pancreatic islets from TG and wt mice fed with HFD, presented as a fold increase over control (n = 3 mice, 15 islets each in duplicate; mean ± SEM). Media used for nonstimulated controls contained 2.8 mM glucose, while the stimulating media contained 16 mM glucose. Unless indicated the presented results were taken from line 85 and the other lines showed similar results.

the pancreas occurs due to lymphocyte infiltration might lead to defective insulin secretion. Histological analysis of the pancreas from mice fed with HFD revealed that 60% of the wt and none of the TG mice had lymphocyte infiltrates in the fat cells surrounding their pancreas (Fig. S2G). Thus, overexpressing SIRT6 protects against many of the manifestations of impaired glucose tolerance associated with HFD.

SIRT6 regulates lipid homeostasis under HFD by down regulating a specific set of PPARγ regulated genes

To explore the mechanism by which SIRT6 protects against the deleterious physiological effects of diet-induced obesity, the transcription profile of visceral fat from MOSES and wt littermates was compared. Pathway analysis (DAVID Bioinformatics Resources) of down regulated genes demonstrated that PPAR signaling was the most affected pathway among all identified KEGG pathways ($P = 3.4 \times 10^{-3}$). PPAR regulated genes are involved in lipid metabolism, lipid transport and adipogenesis. The effect of overexpressing SIRT6 was specific to a set of PPARγ regulated genes, resulting in at least a twofold reduction in their transcription levels (Fig. 5A). Interestingly, no difference was found in the transcription level of PPARγ itself between the TG and wt littermates (Fig. S3A). Of these, selected genes that were previously suggested as potential targets for the metabolic syndrome therapy were validated by quantitative real-time PCR. The transcription levels of these genes were measured from two TG lines. From each line, we examined ten mice, five TG and five wt littermates. Significant reductions in the transcription of angiopoietin-like protein 4 (ANGPTL4), and adipocyte fatty acid-binding protein (A-FABP) were found in the TG mice in comparison to their wt littermates (Fig. 5B). ANGPTL4 is a negative regulator of lipoprotein lipase (LPL) (Yoshida *et al.*, 2002). LPL hydrolyzes serum triglycerides into FFA, allowing their clearance from the circulation. Thus, reduced levels of ANGPTL4 are expected to enhance triglyceride clearance.

The regulation of lipogenesis by PPARγ encouraged us to follow the cycle of triglyceride synthesis and hydrolysis inside the adipose tissues. Quantitative real-time PCR demonstrated that the level of hormone sensitive lipase (HSL), which hydrolyzes triglycerides, did not change (Fig. 5C). However, the levels of DGAT1, a key enzyme in triglycerides synthesis (Cases *et al.*, 1998), were reduced up to 50% in MOSES mice (Fig. 5C). These findings suggest that SIRT6 binds to the DGAT1 promoter and represses its transcription. Indeed chromatin immunoprecipitation (ChIP) assays on DGAT1 promoter show that SIRT6 binds to DGAT1 promoter (Fig. 5D and Fig. S3B), and its binding was 3.5 times higher in MOSES mice than in wt mice. ChIP assay revealed that PPARγ does not bind to DGAT1 promoter (Fig. S3C). Thus, the binding of SIRT6 to DGAT1 promoter did not require the presence of PPARγ on DGAT1 promoter.

Taken together, under HFD conditions, overexpression of SIRT6 increases serum triglyceride clearance and reduces triglyceride synthesis inside adipose tissue by specific inhibition of selected PPAR target genes and DGAT1.

Discussion

Mice deficient in SIRT6 develop abnormalities usually associated with premature aging phenotypes, including severe metabolic defects. Thus, SIRT6 might regulate mammalian longevity via its effect on metabolism. To further examine this possibility we generated a series of TG mice (MOSES lines) overexpressing SIRT6, and followed the effects of overexpressing SIRT6 on fat and glucose metabolism. We show here that SIRT6 overexpression did not cause any metabolic phenotypes in mice fed normal chow other than a decrease in LDL-cholesterol levels. However, SIRT6 overexpression in mice fed a HFD led to the following changes: (i) When fed with HFD, MOSES mice accumulated less total body fat and significantly less visceral fat, triglycerides and LDL-cholesterol than wt animals; (ii) over a 4-month period of HFD, MOSES mice maintained better glucose tolerance than wt littermates due to improved insulin secretion; (iii) overexpression of SIRT6 resulted in a reduction in the transcription of specific PPARγ regulated genes such as ANGPTL4 and A-FABP; and (iv) in comparison to wt mice, MOSES mice exhibited an increase in SIRT6 binding to DGAT1 promoter and a 50% reduction in DGAT1 transcription levels. Taken together, these findings suggest that overexpression of SIRT6 protects against HFD-induced metabolic damage and maintains proper fat and glucose homeostasis by reducing specific PPAR regulated pathways; in particular SIRT6 overexpression increases triglyceride clearance in the blood and reduces production of triglycerides in the adipose tissues (Fig. 5E).

Central obesity and dyslipidemia are considered as major requirements for diagnosing the metabolic syndrome (Huang, 2009). MOSES mice fed a chronic HFD showed a significant improvement in these criteria, highlighting the therapeutic importance of our findings. The combination of the reduction in specific PPARγ regulated genes such as ANGPTL4, together with the reduction in DGAT1, can explain the protection against the increase in triglycerides and abdominal fat induced by HFD. For example, in a mouse model of obesity, ANGPTL4 levels are elevated (Yoon *et al.*, 2000), resulting in increased LPL inhibition. This in turn decreases the clearance of triglycerides from the serum (Yoshida *et al.*, 2002). Therefore, the observed reduction in ANGPTL4 levels in mice overexpressing SIRT6 is expected to result in an opposite phenotype of enhanced clearance of lipoproteins from the serum, and to explain their lower levels in MOSES mice. In addition, reduced levels of DGAT1 result in decreased accumulation of triglycerides in the visceral fat, and can explain the significantly lower percentage of abdominal fat in MOSES mice. Reduction in fat deposits and circular lipids results in improved function of beta cells and improved glucose tolerance, as were indeed seen in the MOSES mice fed HFD. In addition to these effects on transcription, SIRT6 can also

mediate its protective effect against HFD-induced physiological damage via direct deacetylation, thereby modifying the activity of key proteins in fat homeostasis.

ANGPTL4, A-FABP, and DGAT1 were suggested as potential targets for drugs that would control or reverse the metabolic syndrome (Oike *et al.*, 2005; Kusunoki *et al.*, 2006; Furuhashi &

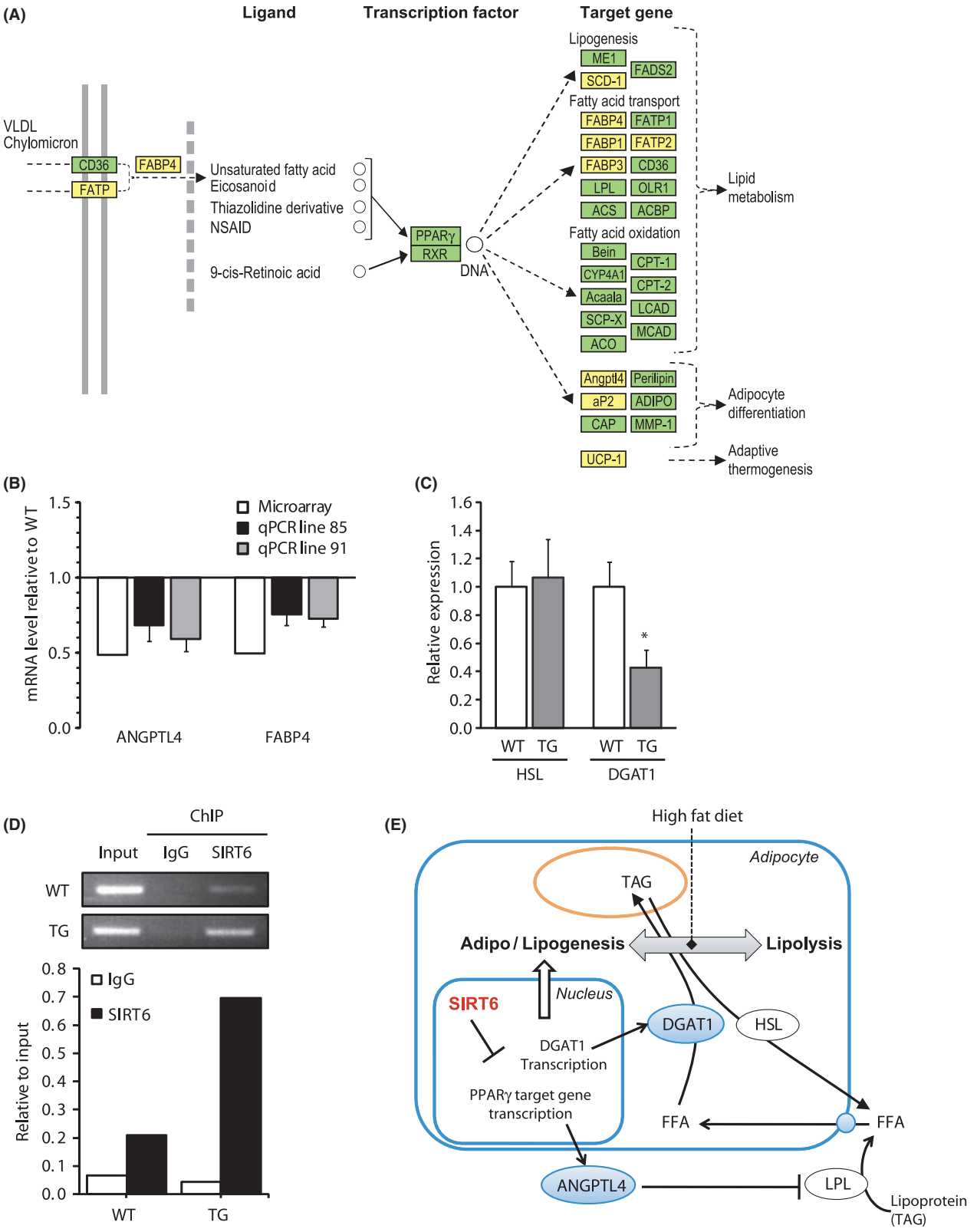

Hotamisligil, 2008). Our data demonstrate that overexpressing SIRT6 results in a reduction in the expression of these genes, and SIRT6 protects against metabolic damage induced by HFD. Thus, developing small molecule activators of SIRT6 has great therapeutic potential. Such molecules have been developed for SIRT1, and are able to mimic the protective effect of overexpressing SIRT1 against obesity-induced physiological damage (Baur *et al.*, 2006; Lagouge *et al.*, 2006; Milne *et al.*, 2007; Feige *et al.*, 2008). Yet, the main difficulty in screening for such molecules is the poor deacetylase activity of SIRT6 *in vitro* (Liszt *et al.*, 2005). Therefore, one of the future challenges in SIRT6 biology would be the development of a reliable *in vitro* deacetylase activity assay for SIRT6; such experiments are currently underway in our lab.

Mice deficient in SIRT1 do not show the same spectrum of phenotypes as mice deficient in SIRT6, but rather develop retinal and heart defects, and rarely survive postnatally (Cheng *et al.*, 2003). Since the absence of each SIRT independently results in premature death, SIRT1 and SIRT6 do not complement each other. Moreover, MOSES and wt mice have similar SIRT1 levels in the liver, WAT, and muscle (Fig. S4A,B). Yet, a comparison of the effects of overexpressing SIRT1 to those of overexpressing SIRT6 reveals similarity between the functions of these proteins. SIRT1 and SIRT6 protect against obesity-induced physiological and metabolic damage, and maintain improved glucose tolerance after several months of HFD (Pfluger *et al.*, 2008). Both negatively regulate the NF-kappaB pathway (Yeung *et al.*, 2004; Kawahara *et al.*, 2009), have been implicated in regulating the role of WRN in telomere maintenance (Li *et al.*, 2008; Michishita *et al.*, 2008) and their protein levels increased in rats fed with CR diet (Cohen *et al.*, 2004; Kanfi *et al.*, 2008b).

Interestingly, at the mechanistic level, SIRT1 and SIRT6 proteins might share functional redundancy, but not necessarily substrate identity. They negatively regulate NFκB by different means. SIRT1 negatively regulates NF-kappaB pathway by deacetylating RelA (Yeung *et al.*, 2004), and SIRT6 attenuates NF-kappaB signaling by deacetylating H3K9 at NFκB/RelA target gene promoters (Kawahara *et al.*, 2009). Furthermore, SIRT1 directly interacts with WRN, whereas SIRT6 does not (Li *et al.*, 2008; Michishita *et al.*, 2008). Similarly, SIRT1 suppresses a different set of PPARγ regulated genes than SIRT6 (Fig. 5A and Wang *et al.*, 2008). The mechanism by which SIRT6 is directed to this specific set of PPARγ target genes and not to others is still elusive. Previous studies localized SIRT6 to the chromatin but did not address how SIRT6 becomes associated with specific loci (Mostoslavsky *et al.*, 2006). We predict that in analogy to SIRT1, which represses PPARγ in association with NcoR and SMART (Picard *et al.*, 2004), the repression of genes by SIRT6 is also complex-dependent. Thus, identification of SIRT6-associated complexes that mediate its protective role against fat-related metabolic defects has great therapeutic implications.

Several conclusions can be drawn from the functional similarity between SIRT1 and SIRT6. These findings strongly suggest that to mimic the beneficial effects of CR on metabolism and life span or to protect against HFD-induced damage, both SIRT1 and SIRT6 should be activated, potentially in addition to other sirtuins, as well. For example, in contrast to SIRT1 overexpression, SIRT6 reduced cholesterol and triglyceride levels under HFD (Pfluger *et al.*, 2008 and Fig. 3B,D). Yet, overexpression of SIRT1 but not SIRT6 increases insulin sensitivity (Pfluger *et al.*, 2008). This might also explain why genetic overexpression of SIRT1 or its activation by resveratrol results in only a limited spectrum of the CR phenotypes and does not extend mice life span (Bordone *et al.*, 2007; Pearson *et al.*, 2008). These findings also suggest that therapeutic approaches for treating the metabolic syndrome must use activators of both SIRT1 and SIRT6. For example, resveratrol might not be sufficient as a monotherapy, as we could not activate SIRT6 deacetylase activity in an *in vitro* assay by using resveratrol (data not shown). Whereas SIRT1 regulates various pathways by deacetylating a wide range of substrates, it appears that SIRT6 executes its regulatory effects only by controlling transcription/chromatin modifications. Our findings that SIRT6 affects the transcription of PPARγ regulated genes, join the recent publications reporting negative regulation by SIRT6 of the transcription of NF-kappaB target genes, and its deacetylation of telomeric chromatin (Kawahara *et al.*, 2009). The functional similarities between SIRT1 and SIRT6 also suggest that other SIRT1 regulated pathways will be recognized in the future to be regulated by SIRT6, as well.

Calorie restriction and metabolic syndrome result in phenotypes that reside at opposite ends of the same continuum. Here, we show that overexpressing SIRT6 blocks the physiological damage caused by diet-induced obesity. These findings, taken together with our previous report demonstrating that SIRT6 levels are induced by CR diet (Kanfi *et al.*, 2008b), might

Fig. 5 SIRT6 overexpression represses the expression of selected PPARγ target genes and key lipid metabolism genes. (A) Modified presentation of PPAR signaling pathway based on KEGG-Cellular Pathways, integrating the gene expression data of adipose tissues from MOSES (TG) vs. wt littermates fed with high fat diet (HFD). Yellow boxes indicate down regulation of expression in TG samples. Green boxes indicate that the gene was not altered. (B) Comparison between cDNA microarray analysis and quantitative real-time RT-PCR of PPARγ and two of its target genes, angiopoietin-like protein 4 (ANGPTL4) and adipocyte fatty acid-binding protein (FABP4) in lines 85 and 91 (n = 5 per group, mean ± SEM). (C) Relative expression of key lipid metabolism genes hormone sensitive lipase and diacylglycerol acyltransferase 1 (DGAT1) analyzed by real-time PCR (n = 5 per group, mean ± SEM) in wt and MOSES mice fed with HFD. (D) ChIP analysis of cross-linked chromatin from adipose tissue of wt and MOSES mice (line 85) fed with HFD. Chromatin fragments were immunoprecipitated with anti-SIRT6 or control antibody (IgG). DNA from input and immunoprecipitated samples were detected by PCR using primers for DGAT1 promoter and separated on agarose gel. A graph representing the difference between the binding of SIRT6 to DGAT1 promoter in wt and TG mice is shown below. (E) Model for the effects of SIRT6 overexpression in adipose tissue of mice under high fat diet; chronic high fat feeding results in an altered lipogenic/lipolytic balance. SIRT6 overexpression inhibits the expression of DGAT1 and selective PPARγ target genes. Two of those genes are the key enzyme in triglyceride synthesis DGAT1 and ANGPTL4 that regulate serum triglycerides clearance by inhibiting lipoprotein lipase. The combination of the reduction in the levels of these proteins will result in a decrease in central obesity and dyslipidemia, two fundamental criteria of the metabolic syndrome. FFA, free fatty acids; TAG, triglycerides.

implicate SIRT6 as a positive regulator of life span by mimicking several aspects of CR. In young mice fed with standard chow diet, we did not find significant effects of SIRT6 on fat and glucose homeostasis. Yet, one cannot rule out that positive effects of overexpressing SIRT6 will become evident in middle aged to elderly animals. The metabolic defects characterizing this time period in the life span of mice resemble the observed phenotypes of mice with metabolic syndrome. Thus, we predict that MOSES mice fed normal chow diet will exhibit some effects of CR in middle age, and will demonstrate extended life span relative to that of their wt littermates.

Experimental procedures

Generation of transgenic mice

SIRT6 mRNA was isolated from C57BL/6J male mouse brain tissue. The complete mouse SIRT6 cDNA was cloned into a pCAGGS plasmid attached to CMV enhancer and chicken β-actin promoter [Prof. J. Miyazaki, Osaka University (Niwa *et al.*, 1991)]. Linearized SIRT6 construct was microinjected into CB6/F1 zygotes. The pronuclear microinjection was carried out by the Department of Veterinary Resources, Weizmann Institute of Science, Israel. For genotyping, DNA was isolated from tails of mice according to the manufacturer's protocol (5Prime, Gaithersburg, MD, USA) and amplified by PCR using the following primers for TG mice genotyping: Sense: 5′-GAG CTG CAC GGA AAC ATG-3′; Antisense: 5′-CCC ATA ATT TTT GGC AGA GG-3′ (unique to the 3′UTR).

Mice housing and diets

Mice were kept under specific pathogen free and 12 h day/night conditions. The mice were divided into two diet groups. Each group was fed a standard chow diet (21 kcal% Protein, 53.5 kcal% Carbohydrate, 4 kcal% Fat) for the first 8 weeks after weaning, and then was fed for 16 weeks with either a standard diet or a HFD (18.4 kcal% Protein, 21.3 kcal% Carbohydrate, 60.3 kcal% Fat) (Teklad TD06414; Harlan, Indianapolis, IN, USA).

Food intake, oxygen consumption, and body composition

Food intake of mice fed with chow or HFD was measured every 24 h, for 4 days. Oxygen consumption (VO_2) and carbon dioxide production (VCO_2) were measured using a specialized cage adjusted for these measurements. The RQ was calculated as the ratio of VCO_2 produced/VO_2 consumed. Body composition was analyzed by DEXA using a Lunar PIXImus densitometer.

Blood parameters

Leptin (R&D, Minneapolis, MN, USA) and insulin (Crystal Chem, Downers Grove, IL, USA) were analyzed from serum by ELISA. FFA in serum were quantified by enzyme-based method (MBL, Woburn, MA, USA). Triglycerides, cholesterol, LDL, and HDL levels were measured directly in whole blood using Lipid Panel Test Strips and CardioCheck analyzer (PTS, Indianapolis, IN, USA).

Metabolic studies

For GTT, the TG mice and their control littermates were subjected to overnight fasting and injected intraperitoneally (IP) with 2 g of glucose per kg of body weight. Blood glucose was measured on samples obtained by tail bleeding prior to glucose administration and after 15, 30, 60, 90, and 120 min using a Ascensia Elite glucose meter (Bayer, Leverkusen, Germany). For ITT mice were fasted for 6 h, injected IP with insulin (0.75 U kg^{-1} body weight) (Eli Lilly, Indianapolis, IN, USA), and blood glucose levels were measured before, and 15, 30, 60, 90, and 120 min after the injection. HOMA of insulin resistance (HOMA-IR) was calculated using the equation: [fasting glucose (mmol L^{-1}) × fasting insulin (microunits mL^{-1})/22.5]. GSIS by isolated pancreatic islets was measured as previously described (Moynihan *et al.*, 2005). Briefly, islets of similar size were hand-picked into groups of 15 islets in duplicate and incubated with Krebs-Ringer bicarbonate HEPES buffer (KRBH) containing either 2.8 mM or 16 mM glucose for 1 h at 37°C and the supernatant was assayed for insulin.

Western blot analysis

Tissues were collected and frozen in liquid nitrogen. Protein was extracted from tissues by homogenization in lysis buffer [50 mM Tris HCl pH 7.5, 150 mM NaCl, 1 mM EDTA, 10% Glycerol, 1%Triton-X100, 0.5%NP40, and Proteinase Inhibitor cocktail tablet (Roche Diagnostics, Switzerland)]. Standard SDS–PAGE electrophoresis was performed. Immunoblotting was carried out with antibodies against SIRT6 (Novus, Littleton, CO, USA), SIRT1 (Abcam, Cambridge, UK) and α-tubulin (12G10 Hybridoma Bank, University of Iowa, USA).

Microarray analysis

Total RNA was extracted using RNeasy kit (Qiagen, Hilden, Germany) from adipose tissue of TG mice and their control littermates fed with normal chow or HFD. After determining the RNA quality and integrity, the isolated total RNA was amplified and fluorescently labeled with Cyanine 3 or Cyanine 5 and repurified using Qiagen's RNeasy Kit. For each hybridization, 1 μg of labeled cRNA were fragmented and hybridized to an Agilent Technologies whole mouse genome Gene Expression Microarray, using the Agilent Gene Expression hybridization kit as described in the manufacturer's manual. Following hybridization, all microarrays were washed and scanned using Agilent's dual laser DNA microarray scanner. The data were then extracted from images by using Feature Extraction 9.1 software (Agilent, Santa Clara, CA, USA). The data were analyzed using GeneSpring GX software (Agilent). Array normalization was performed using intensity-dependent Lowess normalization method.

Quantitative real-time PCR

Total RNA was extracted using RNeasy kit according to the manufacturer's protocol. To remove potential template DNA, the samples were treated with DNase (Qiagen). cDNA was generated using SuperScript Vilo (Invitrogen, Carlsbad, CA, USA). Quantitative real-time PCR was performed in triplicate using ABsolute blue SYBR Green (Thermo, Waltham, MA, USA) in a Chromo4 instrument cycler (Bio-Rad, Hercules, CA, USA). Ct values were normalized to GAPDH. Primer sequences are detailed in Table S2.

Chromatin immunoprecipitation

White adipose tissue samples were treated using an EpiQuik tissue ChIP kit according to the manufacturer's instructions (Epigentek Group Inc., Brooklyn, NY, USA). Briefly, the tissue was mixed with formaldehyde at a final concentration of 1% for 20 min at room temperature to cross-link protein to DNA. Tissue was homogenized using 20 strokes of a Dounce homogenizer. DNA cross-linked with protein was sonicated into fragments of 500–1000 bp. Chromatin fragments were immunoprecipitated with anti-SIRT6 (Sigma-Aldrich, Rehovot, Israel), anti-PPARγ (Santa Cruz Biotechnology, Santa Cruz, CA, USA) or control (IgG) antibody (Epigentek Group Inc.). PCR amplification was performed using primers specific for the DGAT1 promoter (sense, 5′-GAC ATC GGT GCC ATC TCT TT-3′; antisense, 5′-TGA ATC CAC ACC ATC CAA GA-3′) or aP2 promoter (sense, 5′-GAA TTC CAG CAG GAA TCA GG-3′; antisense, 5′-GCC AAA GAG ACA GAG GGC G-3′).

Histopathology

Tissues were fixed in 4% buffered formaldehyde, embedded in paraffin, sectioned and stained with Hematoxylin–Eosin (H&E) stain, or frozen and stained with oil red O stain.

Statistical analysis

Results were expressed as mean ± SEM. *P*-values were calculated by two tailed, unpaired Student's *t*-tests. All measurements were performed in multiple lines. Unless indicated the presented results were taken from line no. 85 and the other lines showed similar results.

Acknowledgments

We thank Doron Ginsberg, Shelley Schwarzbaum (BIU, Israel) and members of the Cohen lab for their helpful comments on the manuscript. We also thank. J. Miyazaki (Osaka U., Japan) for pCAGGS plasmid, Amos Ar (TAU, Israel) for technical advices and Shay Shemesh (BIU, Israel) for technical assistance. This study was supported by grants from the Israeli Academy of Sciences, Binational US-Israel Science Foundation, Israel Cancer Association, Koret Foundation, the Israel Cancer Research Fund, the Israeli Ministry of Health and the ERC: European Research Council.

References

Baur JA, Pearson KJ, Price NL, Jamieson HA, Lerin C, Kalra A, Prabhu VV, Allard JS, Lopez-Lluch G, Lewis K, Pistell PJ, Poosala S, Becker KG, Boss O, Gwinn D, Wang M, Ramaswamy S, Fishbein KW, Spencer RG, Lakatta EG, Le Couteur D, Shaw RJ, Navas P, Puigserver P, Ingram DK, de Cabo R, Sinclair DA (2006) Resveratrol improves health and survival of mice on a high-calorie diet. *Nature* **444**, 337–342.

Blander G, Guarente L (2004) The Sir2 family of protein deacetylases. *Annu. Rev. Biochem.* **73**, 417–435.

Bordone L, Cohen D, Robinson A, Motta MC, van Veen E, Czopik A, Steele AD, Crowe H, Marmor S, Luo J, Gu W, Guarente L (2007) SIRT1 transgenic mice show phenotypes resembling calorie restriction. *Aging Cell* **6**, 759–767.

Burt AD, Mutton A, Day CP (1998) Diagnosis and interpretation of steatosis and steatohepatitis. *Semin. Diagn. Pathol.* **15**, 246–258.

Cases S, Smith SJ, Zheng YW, Myers HM, Lear SR, Sande E, Novak S, Collins C, Welch CB, Lusis AJ, Erickson SK, Farese RV Jr (1998) Identification of a gene encoding an acyl CoA:diacylglycerol acyltransferase, a key enzyme in triacylglycerol synthesis. *Proc. Natl Acad. Sci. USA* **95**, 13018–13023.

Chen D, Steele AD, Lindquist S, Guarente L (2005) Increase in activity during calorie restriction requires Sirt1. *Science* **310**, 1641.

Cheng HL, Mostoslavsky R, Saito S, Manis JP, Gu Y, Patel P, Bronson R, Appella E, Alt FW, Chua KF (2003) Developmental defects and p53 hyperacetylation in Sir2 homolog (SIRT1)-deficient mice. *Proc. Natl Acad. Sci. USA* **100**, 10794–10799.

Cohen HY, Miller C, Bitterman KJ, Wall NR, Hekking B, Kessler B, Howitz KT, Gorospe M, de Cabo R, Sinclair DA (2004) Calorie restriction promotes mammalian cell survival by inducing the SIRT1 deacetylase. *Science* **305**, 390–392.

Feige JN, Lagouge M, Canto C, Strehle A, Houten SM, Milne JC, Lambert PD, Mataki C, Elliott PJ, Auwerx J (2008) Specific SIRT1 activation mimics low energy levels and protects against diet-induced metabolic disorders by enhancing fat oxidation. *Cell Metab.* **8**, 347–358.

Fontana L, Klein S (2007) Aging, adiposity, and calorie restriction. *JAMA* **297**, 986–994.

Frossard JL, Lescuyer P, Pastor CM (2009) Experimental evidence of obesity as a risk factor for severe acute pancreatitis. *World J. Gastroenterol.* **15**, 5260–5265.

Furuhashi M, Hotamisligil GS (2008) Fatty acid-binding proteins: role in metabolic diseases and potential as drug targets. *Nat Rev Drug Discov.* **7**, 489–503.

Grundy SM, Cleeman JI, Daniels SR, Donato KA, Eckel RH, Franklin BA, Gordon DJ, Krauss RM, Savage PJ, Smith SC Jr, Spertus JA, Costa F (2005) Diagnosis and management of the metabolic syndrome: an American Heart Association/National Heart, Lung, and Blood Institute Scientific Statement. *Circulation* **112**, 2735–2752.

Guarente L (2006) Sirtuins as potential targets for metabolic syndrome. *Nature* **444**, 868–874.

Haigis MC, Mostoslavsky R, Haigis KM, Fahie K, Christodoulou DC, Murphy AJ, Valenzuela DM, Yancopoulos GD, Karow M, Blander G, Wolberger C, Prolla TA, Weindruch R, Alt FW, Guarente L (2006) SIRT4 inhibits glutamate dehydrogenase and opposes the effects of calorie restriction in pancreatic beta cells. *Cell* **126**, 941–954.

Huang PL (2009) A comprehensive definition for metabolic syndrome. *Dis. Model Mech.* **2**, 231–237.

Imai S, Johnson FB, Marciniak RA, McVey M, Park PU, Guarente L (2000) Sir2: an NAD-dependent histone deacetylase that connects chromatin silencing, metabolism, and aging. *Cold Spring Harb. Symp. Quant. Biol.* **65**, 297–302.

Kaeberlein M, McVey M, Guarente L (1999) The SIR2/3/4 complex and SIR2 alone promote longevity in *Saccharomyces cerevisiae* by two different mechanisms. *Genes Dev.* **13**, 2570–2580.

Kanfi Y, Peshti V, Gozlan YM, Rathaus M, Gil R, Cohen HY (2008a) Regulation of SIRT1 protein levels by nutrient availability. *FEBS Lett.* **582**, 2417–2423.

Kanfi Y, Shalman R, Peshti V, Pilosof SN, Gozlan YM, Pearson KJ, Lerrer B, Moazed D, Marine JC, De Cabo R, Cohen HY (2008b) Regulation of SIRT6 protein levels by nutrient availability. *FEBS Lett.* **582**, 543–548.

Kawahara TL, Michishita E, Adler AS, Damian M, Berber E, Lin M, McCord RA, Ongaigui KC, Boxer LD, Chang HY, Chua KF (2009) SIRT6 links histone H3 lysine 9 deacetylation to NF-kappaB-dependent gene expression and organismal life span. *Cell* **136**, 62–74.

Kusunoki J, Kanatani A, Moller DE (2006) Modulation of fatty acid metabolism as a potential approach to the treatment of obesity and the metabolic syndrome. *Endocrine* **29**, 91–100.

Lagouge M, Argmann C, Gerhart-Hines Z, Meziane H, Lerin C, Daussin F, Messadeq N, Milne J, Lambert P, Elliott P, Geny B, Laakso M, Puigserver P, Auwerx J (2006) Resveratrol improves mitochondrial function and protects against metabolic disease by activating SIRT1 and PGC-1alpha. *Cell* **127**, 1109–1122.

Li K, Casta A, Wang R, Lozada E, Fan W, Kane S, Ge Q, Gu W, Orren D, Luo J (2008) Regulation of WRN protein cellular localization and enzymatic activities by SIRT1-mediated deacetylation. *J. Biol. Chem.* **283**, 7590–7598.

Lin SJ, Defossez PA, Guarente L (2000) Requirement of NAD and SIR2 for life-span extension by calorie restriction in *Saccharomyces cerevisiae*. *Science* **289**, 2126–2128.

Liszt G, Ford E, Kurtev M, Guarente L (2005) Mouse Sir2 homolog SIRT6 is a nuclear ADP-ribosyltransferase. *J. Biol. Chem.* **280**, 21313–21320.

McCay CM, Crowell MF, Maynard LA (1935) The effect of retarded growth upon the length of life span and upon the ultimate body size. *J. Nutr.* **10**, 63–79.

Michishita E, McCord RA, Berber E, Kioi M, Padilla-Nash H, Damian M, Cheung P, Kusumoto R, Kawahara TL, Barrett JC, Chang HY, Bohr VA, Ried T, Gozani O, Chua KF (2008) SIRT6 is a histone H3 lysine 9 deacetylase that modulates telomeric chromatin. *Nature* **452**, 492–496.

Milionis HJ, Florentin M, Giannopoulos S (2008) Metabolic syndrome and Alzheimer's disease: a link to a vascular hypothesis? *CNS Spectr.* **13**, 606–613.

Milne JC, Lambert PD, Schenk S, Carney DP, Smith JJ, Gagne DJ, Jin L, Boss O, Perni RB, Vu CB, Bemis JE, Xie R, Disch JS, Ng PY, Nunes JJ, Lynch AV, Yang H, Galonek H, Israelian K, Choy W, Iffland A, Lavu S, Medvedik O, Sinclair DA, Olefsky JM, Jirousek MR, Elliott PJ, Westphal CH (2007) Small molecule activators of SIRT1 as therapeutics for the treatment of type 2 diabetes. *Nature* **450**, 712–716.

Mostoslavsky R, Chua KF, Lombard DB, Pang WW, Fischer MR, Gellon L, Liu P, Mostoslavsky G, Franco S, Murphy MM, Mills KD, Patel P, Hsu JT, Hong AL, Ford E, Cheng HL, Kennedy C, Nunez N, Bronson R, Frendewey D, Auerbach W, Valenzuela D, Karow M, Hottiger MO, Hursting S, Barrett JC, Guarente L, Mulligan R, Demple B, Yancopoulos GD, Alt FW (2006) Genomic instability and aging-like phenotype in the absence of mammalian SIRT6. *Cell* **124**, 315–329.

Moynihan KA, Grimm AA, Plueger MM, Bernal-Mizrachi E, Ford E, Cras-Meneur C, Permutt MA, Imai S (2005) Increased dosage of mammalian Sir2 in pancreatic beta cells enhances glucose-stimulated insulin secretion in mice. *Cell Metab.* **2**, 105–117.

Nemoto S, Fergusson MM, Finkel T (2004) Nutrient availability regulates SIRT1 through a forkhead-dependent pathway. *Science* **306**, 2105–2108.

Niwa H, Yamamura K, Miyazaki J (1991) Efficient selection for high-expression transfectants with a novel eukaryotic vector. *Gene* **108**, 193–199.

Oike Y, Akao M, Kubota Y, Suda T (2005) Angiopoietin-like proteins: potential new targets for metabolic syndrome therapy. *Trends Mol. Med.* **11**, 473–479.

Pearson KJ, Baur JA, Lewis KN, Peshkin L, Price NL, Labinskyy N, Swindell WR, Kamara D, Minor RK, Perez E, Jamieson HA, Zhang Y, Dunn SR, Sharma K, Pleshko N, Woollett LA, Csiszar A, Ikeno Y, Le Couteur D, Elliott PJ, Becker KG, Navas P, Ingram DK, Wolf NS, Ungvari Z, Sinclair DA, de Cabo R (2008) Resveratrol delays age-related deterioration and mimics transcriptional aspects of dietary restriction without extending life span. *Cell Metab.* **8**, 157–168.

Pfluger PT, Herranz D, Velasco-Miguel S, Serrano M, Tschop MH (2008) Sirt1 protects against high-fat diet-induced metabolic damage. *Proc. Natl Acad. Sci. USA* **105**, 9793–9798.

Picard F, Kurtev M, Chung N, Topark-Ngarm A, Senawong T, Machado De Oliveira R, Leid M, McBurney MW, Guarente L (2004) Sirt1 promotes fat mobilization in white adipocytes by repressing PPAR-gamma. *Nature* **429**, 771–776.

Rogina B, Helfand SL (2004) Sir2 mediates longevity in the fly through a pathway related to calorie restriction. *Proc. Natl Acad. Sci. USA* **101**, 15998–16003.

Tissenbaum HA, Guarente L (2001) Increased dosage of a sir-2 gene extends lifespan in *Caenorhabditis elegans*. *Nature* **410**, 227–230.

Wang H, Qiang L, Farmer SR (2008) Identification of a domain within peroxisome proliferator-activated receptor gamma regulating expression of a group of genes containing fibroblast growth factor 21 that are selectively repressed by SIRT1 in adipocytes. *Mol. Cell. Biol.* **28**, 188–200.

Weindruch R, Walford RL (1988) *The Retardation of Aging and Disease by Dietary Restriction*, Springfield, IL, USA: Thomas.

Yeung F, Hoberg JE, Ramsey CS, Keller MD, Jones DR, Frye RA, Mayo MW (2004) Modulation of NF-kappaB-dependent transcription and cell survival by the SIRT1 deacetylase. *EMBO J.* **23**, 2369–2380.

Yoon JC, Chickering TW, Rosen ED, Dussault B, Qin Y, Soukas A, Friedman JM, Holmes WE, Spiegelman BM (2000) Peroxisome proliferator-activated receptor gamma target gene encoding a novel angiopoietin-related protein associated with adipose differentiation. *Mol. Cell. Biol.* **20**, 5343–5349.

Yoshida K, Shimizugawa T, Ono M, Furukawa H (2002) Angiopoietin-like protein 4 is a potent hyperlipidemia-inducing factor in mice and inhibitor of lipoprotein lipase. *J. Lipid Res.* **43**, 1770–1772.

Supporting Information

Additional supporting information may be found in the online version of this article:

Fig. S1 Body composition.

Fig. S2 Additional metabolic characteristics.

Fig. S3 Relative expression of PPARγ and the binding of SIRT6 and PPARγ to diacylglycerol acyltransferase 1 promoter in adipose tissue.

Fig. S4 SIRT1 expression in wild-type and transgenic mice.

Table S1 MOSES mice mRNA levels relative to wt littermates

Table S2 Primer sequences for quantitative real-time polymerase chain reaction

As a service to our authors and readers, this journal provides supporting information supplied by the authors. Such materials are peer-reviewed and may be re-organized for online delivery, but are not copy-edited or typeset. Technical support issues arising from supporting information (other than missing files) should be addressed to the authors.